

Rapid Energy Transfer in Cascade-Type Bodipy Dyes

Anthony Harriman,^{*,†} Guillaume Izzet,[†] and Raymond Ziessel^{*,‡}

Contribution from the Molecular Photonics Laboratory, School of Natural Sciences, Bedson Building, University of Newcastle, Newcastle upon Tyne NE1 7RU, United Kingdom, and Laboratoire de Chimie Moléculaire, Ecole de Chimie, Polymères et Matériaux, CNRS, 25 rue Becquerel, 67087 Strasbourg Cedex 02, France

Received May 5, 2006; E-mail: anthony.harriman@ncl.ac.uk; ziessel@chimie.u-strasbg.fr

Abstract: Three new molecular dyads, comprising a bora-3a,4a-diaza-s-indacene (Bodipy) dye linked to two aromatic polycycles via the boron center, have been synthesized and fully characterized. The polycyclic compounds are either pyrene or perylene, or a mixture of both. Whereas the absorption spectral profiles contain important contributions from each of the subunits, fluorescence occurs exclusively from the Bodipy fragment. Intramolecular excitation energy transfer is extremely efficient in each case, even though spectral overlap integrals for the pyrene-based system are modest. Although these polycycles are sterically congested, molecular dynamics simulations indicate that they are in dynamic motion, and this hinders proper computation of the orientation factors for Förster-type energy transfer. These new dyes, especially the mixed polycycle system, greatly extend the range of excitation wavelengths that can be used for fluorescence microscopy.

Introduction

An inordinately wide range of bora-3a,4a-diaza-s-indacene (Bodipy) dyes have been reported in the literature and used for such diverse applications as biolabels,¹ artificial light harvesters,² sensitizers for solar cells,³ fluorescent sensors,^{4,5} electroluminescent agents,⁶ laser dyes,⁷ stains for DNA,⁸ drug delivery templates,⁹ and electron-transfer reagents.¹⁰ A common feature for all such applications concerns the intense fluorescence and favorable photophysics of the Bodipy family of dyes.¹¹ A noted weakness of Bodipy dyes, and indeed most other classes of intensely fluorescent dyes, is the small Stokes' shift, which

presents problems when using the dye as a fluorescent reagent in biotechnology.¹² Indeed, it has become increasingly clear that dyes based on a single chromophore are inadequate for purposes such as flow cytometry, fluorescence labeling, and chemical sensing because of the closeness between excitation and detection wavelengths.¹³ This realization has led to the development of dual-chromophore dyes that possess extended "virtual" Stokes' shifts.¹⁴ Several Bodipy-based dual-chromophore dyes have been reported in recent years wherein aromatic polycycles have been appended to the organic framework. These reagents operate by virtue of efficient intramolecular excitation energy transfer from the polycycle to the Bodipy dye, followed by regular fluorescence from the dye. In this way, the energy gap between excitation and detection wavelengths can be increased by at least 10-fold.¹⁵

The most popular aromatic polycycles have been anthracene and pyrene, but in all cases these ancillary chromophores have been attached to the organic core and the difluoroboron unit has been retained.^{16,17} Both through-space and through-bond energy-transfer processes have been described, with the poly-

[†] University of Newcastle.[‡] Ecole de Chimie, Polymères, Matériaux.

- (1) Haugland, R. P. In *The Handbook: A Guide to Fluorescent Probes and Labelling Technologies*, 10th ed.; Spence, M. T. Z., Ed.; Molecular Probes: Eugene, OR, 2005.
- (2) Lokey, G. E.; Hanes, M. S.; Bailey, S. T.; Shearer, J. D. M.; Zhang, Y.-Z.; Wittmershaus, B. P. Presented at the 225th ACS National Meeting, New Orleans, LA, March 23–27, 2003.
- (3) Hattori, S.; Ohkubo, K.; Urano, Y.; Sunahara, H.; Nagano, T.; Wada, Y.; Tkachenko, N. V.; Lemmetyinen, H.; Fukuzumi, S. *J. Phys. Chem. B* **2005**, *109*, 15368.
- (4) (a) Kollmannsberger, M.; Rurack, K.; Resch-Genger, U.; Daub, J. *J. Phys. Chem. A* **1998**, *102*, 10211. (b) Rurack, K.; Kollmannsberger, M.; Resch-Genger, U.; Daub, J. *J. Am. Chem. Soc.* **2000**, *122*, 968. (c) Turfan, B.; Akkaya, E. U. *Org. Lett.* **2002**, *4*, 2857. (d) Gabe, Y.; Urano, Y.; Kikuchi, K.; Kojima, H.; Nagano, T. *J. Am. Chem. Soc.* **2004**, *126*, 3357. (e) Yogo, T.; Urano, Y.; Ishitsuka, Y.; Maniwa, F.; Nagano, T. *J. Am. Chem. Soc.* **2005**, *127*, 12162.
- (5) Goze, C.; Ulrich, G.; Charbonnière, L.; Cesario, M.; Prangé, T.; Ziessel, R. *Chem. Eur. J.* **2003**, *9*, 3748.
- (6) (a) Lai, R. Y.; Bard, A. J. *J. Phys. Chem. B* **2003**, *107*, 5036. (b) Brom, J. M., Jr.; Langer, J. L. *J. Alloys Compd.* **2002**, *338*, 112. (c) Hepp, A.; Ulrich, G.; Schmechel, R.; von Seggern, H.; Ziessel, R. *Synth. Met.* **2004**, *146*, 11.
- (7) (a) Sathyamoorthi, G.; Wolford, L. T.; Haag, A. M.; Boyer, J. H. *Heteroat. Chem.* **1994**, *5*, 245. (b) Chen, T.; Boyer, J. H.; Trudell, M. L. *Heteroat. Chem.* **1997**, *8*, 51.
- (8) Rostron, J. P.; Ulrich, G.; Retailleau, P.; Harriman, A.; Ziessel, R. *New J. Chem.* **2005**, *29*, 1241.
- (9) McCusker, C.; Carroll, J. B.; Rotello, V. M. *Chem. Commun.* **2005**, 996.
- (10) Debrezény, M. P.; Svec, W. A.; Wasielewski, M. R. *Science* **1996**, *274*, 584.

- (11) (a) Burghart, A.; Kim, H.; Welch, M. B.; Thoresen, L. H.; Reibenspies, J.; Burgess, K.; Bergström, F.; Johansson, L. B.-A. *J. Org. Chem.* **1999**, *64*, 7813. (b) Chen, J.; Burghart, A.; Derecskei-Kovacs, A.; Burgess, K. *J. Org. Chem.* **2000**, *65*, 2900. (c) Coskun, A.; Akkaya, E. U. *J. Am. Chem. Soc.* **2005**, *127*, 10464. (d) Bricks, J. L.; Kovalchuk, A.; Trieflinger, C.; Nofz, M.; Büschel, M.; Tolmachev, A. I.; Daub, J.; Rurack, K. *J. Am. Chem. Soc.* **2005**, *127*, 13522.
- (12) Martin, H.; Rudolf, H.; Vlastimil, F., Eds. *Fluorescence Spectroscopy in Biology: Advanced Methods and their Applications to Membranes, Proteins, DNA, and Cells*; Springer-Verlag: Heidelberg, Germany, 2005.
- (13) Ju, J.; Ruan, C.; Fuller, C. W.; Glazer, A. N.; Mathies, R. A. *Proc. Natl. Acad. Sci. U.S.A.* **1995**, *92*, 4347.
- (14) Kang, H. C.; Haugland, R. P. U.S. Patent 5,451,663, Sept 19, 1995.
- (15) Ulrich, G.; Goze, C.; Guardigli, M.; Roda, A.; Ziessel, R. *Angew. Chem., Int. Ed.* **2005**, *44*, 3694.
- (16) Wan, C.-W.; Burghart, A.; Chen, J.; Bergström, F.; Johansson, L. B.-A.; Wolford, M. F.; Kim, T. G.; Topp, M. R.; Hochstrasser, R. M.; Burgess, K. *Chem. Eur. J.* **2003**, *9*, 4430.

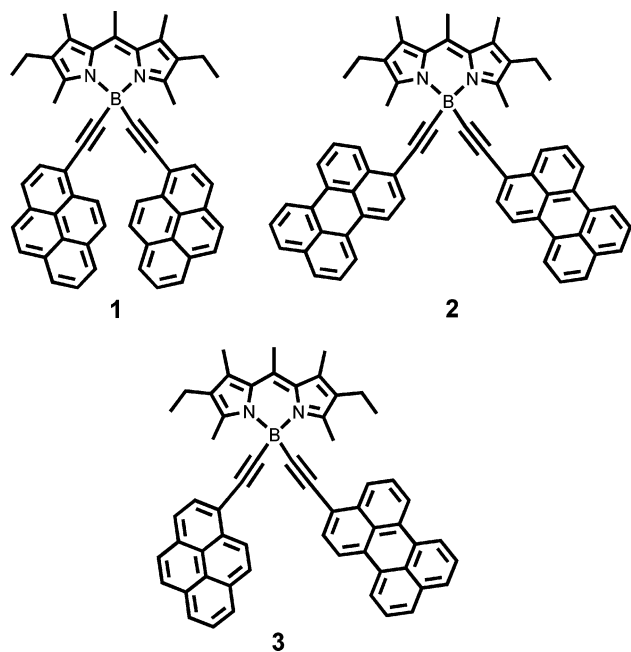


Figure 1. Structural formulas and abbreviations used for the Bodipy-based cascade-type dyes studied in this work.

cycle being attached at different sites on the indacene backbone.¹⁶ Many of these dual-chromophore dyes have connected the subunits by way of ethynylene linkers so as to ensure good electronic communication.¹⁷ We now seek to expand on this subject by introducing a new class of dual-chromophore dyes in which the polycycles replace the fluorine atoms. This strategy places the substituent close to the indacene core and allows for facile synthesis of asymmetrical derivatives bearing two different polycycles. For the compounds described herein, connection to the boron center is made via a single ethyne group. It will be shown that intramolecular singlet energy transfer is extremely efficient and that, in the case of a mixed pyrene/perylene system, the fluorescence excitation spectrum covers most of the region between 200 and 540 nm.

Experimental Methods

Structural formulas for the molecular systems studied herein are given in Figure 1. The new compounds were synthesized and characterized by NMR, fast-atom bombardment mass spectra in positive mode (FAB⁺), Fourier transform infrared (FT-IR), UV–visible spectroscopy, and elemental analysis.

Synthesis. General Methods. The 400 (¹H) and 100.3 (¹³C) MHz NMR spectra were recorded at room temperature using perdeuterated solvents as internal standard: δ (H) in ppm relative to residual protiated solvent; δ (C) in ppm relative to the solvent. A fast-atom bombardment ZAB-HF-VB analytical apparatus, operated in positive mode, was used for mass spectral studies with *m*-nitrobenzyl alcohol (*m*-NBA) as matrix. FT-IR spectra were recorded on the neat liquids or as thin films, prepared with a drop of dichloromethane and evaporated to dryness on KBr pellets. Chromatographic purification was conducted using standardized flash silica gel. Thin-layer chromatography (TLC) was performed on aluminum oxide or silica plates coated with fluorescent indicator. All mixtures of solvents are given as volume/volume (v/v) ratios.

Materials. Tetrahydrofuran was distilled over sodium and benzophenone. Samples of 4,4-difluoro-1,3,5,7,8-pentamethyl-2,4-diethyl-

4-bora-3a,4a-diaza-s-indacene¹⁸ (abbreviated herein as *F*-Bodipy), 1-ethynylpyrene,¹⁹ and 1-ethynylperylene²⁰ were prepared and purified according to literature procedures. *n*-Butyl lithium was titrated prior to use according to a literature procedure.²¹ All reactions were carried out under dry argon using Schlenk-tube and vacuum-line techniques.

Experimental Procedure and Characterization. The pyrene and perylene lithio derivatives were prepared in two separate Schlenk flasks at -78 °C. To a stirred, degassed solution of 1-ethynylpyrene (0.154 g, 0.680 mmol) in anhydrous THF (10 mL), *n*-BuLi titrated at 1.49 N (0.460 mL, 0.680 mmol) was added dropwise, and the mixture was stirred at -78 °C for 1.5 h. In a separate Schlenk tube, 1-ethynylperylene (0.188 g, 0.680 mmol) was dissolved in anhydrous THF (10 mL), *n*-BuLi titrated at 1.49 N (0.460 mL, 0.680 mmol) was added dropwise, and the mixture was stirred at -78 °C for 1 h. After that time, the resulting pyrene anion was transferred via cannula to the perylene solution kept at -78 °C. The resulting solution was transferred rapidly to the difluoroboradiaindacene precursor (0.180 g, 0.566 mmol) dissolved in anhydrous THF (10 mL) and maintained at room temperature. The mixture was stirred at room temperature for 5 min, until complete consumption of the starting material was observed by TLC. Water (1 mL) was then added, and the solution was extracted with CH₂Cl₂ (3 × 50 mL). The organic phase was dried over cotton-wool. After evaporation, the crude mixture was purified by column chromatography on flash silica using cyclohexane and increasing amounts of ethyl acetate (1–20%). The crude reaction mixture was dispersed on neutral alumina and deposited as a solid on the top of the column. The pure compounds were isolated by slow evaporation of dichloromethane from a mixture of dichloromethane, methanol (trace), and hexane.

Characterization of the Compounds. 4,4'-Bis(pyrenyl-1-ethynyl)-1,3,5,7,8-pentamethyl-2,6-diethyl-4-bora-3a,4a-diaza-s-indacene (1). Isolated yield: 20%, 0.099 g. ¹H NMR (CDCl₃): δ = 8.75 (d, 2H, ³J = 9.0 Hz), 8.16–7.96 (m, 16H), 3.11 (s, 6H), 2.74 (s, 3H), 2.56 (q, 4H, ³J = 7.5 Hz), 2.45 (s, 6H), 1.17 (t, 6H, ³J = 7.5 Hz). ¹³C {¹H} NMR (CDCl₃, 100 MHz): δ = 152.1, 140.0, 134.7, 132.8, 132.1, 131.4, 131.3, 130.5, 130.4, 129.7, 127.8, 127.43, 127.38, 126.4, 126.0, 125.3, 125.11, 125.08, 124.61, 124.57, 124.4, 94.4, 17.6, 17.4, 15.2, 14.8, 14.5. IR (KBr mull): ν = 2960 (s), 2293 (m), 2169 (w), 1599 (s), 1430 (s), 1184 (s), 978 (s) cm⁻¹. FAB⁺ (*m/z*, nature of peak, relative intensity): 731.2, [M + H]⁺, 100. Anal. Calcd for C₅₄H₄₃BN₂ (*M_r* = 730.74): C, 88.76; H, 5.93; N, 3.83. Found: C, 88.57; H, 5.77; N, 3.65.

4,4'-Bis(perylene-3-ethynyl)-1,3,5,7,8-pentamethyl-2,6-diethyl-4-bora-3a,4a-diaza-s-indacene (2). Isolated yield: 16%, 0.066 g. Prepared according to the general procedure with 1-ethynylperylene (0.045 g, 0.16 mmol) in 5 mL of THF, 93 μ L of *n*-butyl lithium (1.74 M in *n*-hexane), and **1** (0.026 g, 0.082 mmol) in 10 mL of THF. Complete consumption of the starting material was observed after 30 min. The chromatography was performed on silica (CH₂Cl₂/cyclohexane, 20:80), and recrystallization gave 0.02 g of **2** (15% yield). ¹H NMR (CDCl₃): δ = 8.37 (d, 2H, ³J = 8.1 Hz), 8.21–8.13 (m, 6H), 8.08 (d, 2H, ³J = 8.1 Hz), 7.67–7.65 (m, 4H), 7.61 (d, 2H, ³J = 7.9 Hz), 7.51–7.43 (m, 6H), 3.00 (s, 6H), 2.71 (s, 3H), 2.52 (q, 4H, ³J = 7.5 Hz), 2.43 (s, 6H), 1.13 (t, 6H, ³J = 7.5 Hz). ¹³C {¹H} NMR (CDCl₃): δ = 152.1, 135.4, 134.8, 134.7, 132.9, 131.5, 131.4, 131.3, 130.6, 130.5, 128.7, 127.9, 127.1, 127.0, 126.7, 123.0, 120.63, 120.57, 120.4, 119.9, 17.6, 17.5, 15.3, 14.9, 14.5. IR (KBr): ν = 2922 (m), 2125 (m), 2172 (w), 1618 (m), 1554 (m), 1430 (s), 1184 (s), 1122 (s), 977 (m), 876 (m), 767 (m). FAB⁺ (*m/z*, nature of peak, relative intensity): 831.1,

(18) Shah, M.; Thangaraj, K.; Soong, M. L.; Wolford, L.; Boyer, J. H.; Politzer, I. R.; Pavlopoulos, T. G. *Heteroat. Chem.* **1990**, *1*, 389.

(19) (a) Harriman, A.; Hissler, M.; Khatyr, A.; Ziessel, R. *Chem. Commun.* **1999**, 735. (b) Hissler, M.; Harriman, A.; Khatyr, A.; Ziessel, R. *Chem. Eur. J.* **1999**, *11*, 3366.

(20) Inouye, M.; Hyodo, Y.; Nakazumi, H. *J. Org. Chem.* **1999**, *64*, 2704.

(21) Suffert, J. J. *Org. Chem.* **1989**, *54*, 509.

(17) Ziessel, R.; Goze, C.; Ulrich, G.; Césario, M.; Retaillieu, P.; Harriman, A.; Rostron, J. P. *Chem. Eur. J.* **2005**, *11*, 7366.

$[M + H]^+$, 100. Anal. Calcd for $C_{62}H_{47}BN_2 \cdot 1/2CH_2Cl_2$ ($M_r = 830.86 + 42.46$): C, 85.96; H, 5.54; N, 3.21. Found: C, 85.42; H, 5.51; N, 3.21.

4-(Pyrenyl-1-ethynyl)-4'-(perylene-3-ethynyl)-1,3,5,7,8-pentamethyl-2,6-diethyl-4-bora-3a,4a-diaza-s-indacene (3). Isolated yield: 28%, 0.149 g. 1H NMR ($CDCl_3$): $\delta = 8.64$ (d, 1H, $^3J = 9.0$ Hz), 8.34 (d, 1H, $^3J = 8.0$ Hz), 8.24 (t, 1H, $^3J = 8.0$ Hz), 8.20–8.02 (m, 10H), 7.85 (d, 1H, $^3J = 9.0$ Hz), 7.62 (t, 1H, $^3J = 8.0$ Hz), 7.55–7.48 (m, 5H), 3.05 (s, 3H), 3.01 (s, 3H), 2.80 (s, 3H), 2.60 (q, 2H, $^3J = 7.4$ Hz), 2.57 (q, 2H, $^3J = 7.4$ Hz), 2.51 (s, 3H), 2.49 (s, 3H), 1.19 (t, 3H, $^3J = 7.4$ Hz), 1.16 (t, 3H, $^3J = 7.4$ Hz). $^{13}C\{^1H\}$ NMR ($CDCl_3$): $\delta = 152.2$, 140.1, 137.9, 135.5, 134.7, 134.6, 132.9, 132.3, 131.5, 131.4, 131.3, 130.6, 130.5, 130.4, 129.7, 128.8, 127.8, 127.6, 127.4, 127.3, 126.7, 126.4, 126.1, 125.3, 125.2, 125.0, 124.6, 124.5, 124.3, 124.2, 124.1, 119.8, 94.5, 17.7, 17.6, 17.4, 17.3, 15.3, 15.2, 14.8, 14.7, 14.5. IR (KBr): $\nu = 3043$ (m), 2960 (m), 2926 (m), 2868 (m), 2161 (m), 1597 (m), 1555 (s), 1479 (s), 1386 (m), 1360 (m), 1323 (m), 1184 (s), 1122 (m), 1062 (m), 977 (s), 846 (m). FAB $^+$ (m/z , nature of peak, relative intensity): 781.2, $[M + H]^+$, 100. Anal. Calcd for $C_{58}H_{45}BN_2$ ($M_r = 780.80$): C, 89.22; H, 5.81; N, 3.59. Found: C, 88.94; H, 5.67; N, 3.41.

Spectroscopic Studies. Spectrophotometric grade solvents were purchased from Aldrich Chemical Co. and used as received. Absorption and fluorescence spectra were recorded using a Hitachi U3300 spectrophotometer and a fully corrected Yvon-Jobin Fluorolog Tau-3 spectrofluorimeter, respectively. Low-temperature emission spectra were taken using an immersion-well liquid N_2 Dewar. Emission quantum yields were measured in N_2 -purged 2-methyltetrahydrofuran (MeTHF) relative to Rhodamine 6G (in methanol)²² or Coumarin 153 (in cyclohexane or ethanol/water 1:1).²³ Corrections were made for changes in refractive index²⁴ or density as required. Fluorescence lifetimes were recorded using the phase modulation method on an Yvon-Jobin Fluorolog Tau-3 Lifetime System, with the instrumental response function being measured against a solution of Ludox in distilled water. Additional lifetime measurements were made with a PTI Xenoflash system. All solutions used for fluorescence spectral measurements were optically dilute and were used in conjunction with nonemissive glass cutoff filters.

Flash photolysis studies were made with an Applied Photophysics Ltd. LKS60 instrument. Excitation was made with 4-ns pulses at 532 nm, delivered with a frequency-doubled, Q-switched Nd:YAG laser, while detection was made at 90° using a pulsed, high-intensity Xe arc lamp. The signal was detected with a fast-response photomultiplier tube after passage through a high-radiance monochromator. Transient differential absorption spectra were recorded point-by-point, with five individual records being averaged at each wavelength. Kinetic measurements were made after averaging 50 individual records using global analysis methods. The sample was purged with N_2 before use. For some studies, iodomethane (10% v/v) was added before photolysis. The laser intensity was calibrated by reference to the triplet state of zinc meso-tetraphenylporphyrin in deoxygenated toluene.²⁵

Fast transient spectroscopy was made by pump-probe techniques using femtosecond pulses delivered from a Ti:sapphire generator amplified with a multipass amplifier pumped via the second harmonic of a Q-switched Nd:YAG laser. The amplified pulse energies varied from 0.3 to 0.5 mJ, and the repetition rate was kept at 10 Hz. Part of the beam (ca. 20%) was focused onto a second harmonic generator in order to produce the excitation pulse. The residual output was directed onto a 4-mm sapphire plate so as to create a white light continuum for detection purposes. The continuum was collimated and split into two equal beams. The first beam was used as reference, while the second

beam was combined with the excitation pulse and used as the diagnostic beam. The two beams were directed to different parts of the entrance slit of a cooled charge-coupled device (CCD) detector and used to calculate differential absorbance values. The CCD shutter was kept open for 1 s, and the accumulated spectra were averaged. This procedure was repeated until about 100 individual spectra had been averaged. Time-resolved spectra were recorded with a delay line stepped in increments of 100 fs. The sample, possessing an absorbance of ca. 1 at 420 nm, was flowed through a quartz cuvette (optical path length = 2 mm) and maintained under an atmosphere of N_2 .

Electrochemical studies employed cyclic voltammetry with a conventional three-electrode system using a BAS CV-50W voltammetric analyzer equipped with a Pt microdisk (2 mm²) working electrode and a platinum wire counter electrode. Ferrocene was used as an internal standard and was calibrated against a saturated calomel reference electrode (SCE) separated from the electrolysis cell by a glass frit presoaked with electrolyte solution. Solutions contained the electrode-active substrate (ca. 1.5×10^{-3} M) in solvent previously deoxygenated with anhydrous nitrogen and with tetra-*n*-butylammonium hexafluorophosphate (0.1 M) as supporting electrolyte. The quoted half-wave potentials were reproducible to within ± 15 mV.

Molecular orbital calculations were made on energy-minimized conformations calculated by Gaussian 03 using the parametrized semiempirical AM1 method and checking for imaginary frequencies.²⁶ Several different starting geometries were sampled. Such AM1 calculations are far from definitive for boron-containing compounds but have been found to adequately model cyclic boron ethers.²⁷ Parameters for boron were taken from the literature.²⁸ These calculations were used to generate energy-minimized geometries and transition dipole moments for the dyes in vacuo. Molecular dynamics simulations (MDS) were performed with INSIGHT-II²⁹ running on a Silicon Graphics O2 workstation. Structures were drawn in the Builder module, and partial charges were assigned using the ESFF force field.³⁰ Energy minimization was carried out with the Discover-3 module using the conjugate gradient method with a cutoff of 9.5 Å until the maximum derivative was less than 0.0005 kcal/Å. The energy-minimized geometries were used as the starting points for the MDS studies. Each MDS run consisted of an initial 10 ps of equilibration using the velocity scaling method, followed by 100 ps of production dynamics. During the latter stage, the temperature averaged 300 K, with a standard deviation of 4.8 K. Data points were sampled each 10 fs of simulation time.

Results and Discussion

Synthesis and Characterization. The three target compounds were prepared in a single reaction using the difluoro derivative (*F*-Bodipy) and half an equivalent each of 1-lithioethynylpyrene and 1-lithioethynylperylene. Due to comparable reactivity, it was anticipated that a statistical ratio of the dyes would be formed. Separation of the three compounds was successfully realized on several flash chromatography columns using adequate mobile phases, followed by multiple recrystallizations. The fingerprint of these molecules is given by the proton NMR spectra. In particular, compound **1** exhibits a characteristic doublet at 8.75 ppm, whereas for **2** a doublet is found at 8.37 ppm. In both cases, the integrations of these peaks correspond

(22) Olmsted, J., III. *J. Phys. Chem.* **1979**, *83*, 2581.

(23) Jones, G., II; Rahman, M. A. *J. Phys. Chem.* **1994**, *98*, 13028.

(24) Eaton, D. F. *Pure Appl. Chem.* **1988**, *60*, 1107.

(25) (a) Hurley, J. K.; Sinai, N.; Linschitz, H. *Photochem. Photobiol.* **1983**, *38*, 9. (b) Carmichael, I.; Hug, G. L. *J. Phys. Chem. Ref. Data* **1986**, *15*, 1.

(26) Frisch, M. J.; et al. *Gaussian 03*, revision C.02; Gaussian, Inc.: Wallingford, CT, 2004.

(27) Kuznetsov, V. V. *J. Struct. Chem.* **2001**, *42*, 494.

(28) (a) Dewar, M. J. S.; Reynolds, C. H. *J. Comput. Chem.* **1986**, *2*, 140. (b) Dewar, M. J. S.; Zoebisch, E. G.; Healy, E. F.; Stewart, J. P. *J. Am. Chem. Soc.* **1985**, *107*, 3902. (c) Dewar, M. J. S.; McKee, M. L.; Rzepa, H. S. *J. Am. Chem. Soc.* **1978**, *100*, 3607. (d) Dewar, M. J. S.; Thiel, W. *J. Am. Chem. Soc.* **1977**, *99*, 4899. (e) Dewar, M. J. S.; Jie, C.; Zoebisch, E. G. *Organometallics* **1988**, *7*, 513.

(29) *INSIGHT-II*; Accelrys Software Inc.: Cambridge, UK, 2001–2006.

(30) Shi, S.; Yan, L.; Yang, Y.; Fisher-Shaulsky, J.; Thacher, T. *J. Comput. Chem.* **2003**, *24*, 1059.

to the two protons located at the α position of the ethynyl tether and lying in the deshielding cone of the indacene core. As expected for the mixed pyrene/perylene dye **3**, two doublets, each integrating for one proton, were found at 8.64 and 8.34 ppm. Furthermore, owing to the asymmetry introduced by two different polyaromatic nuclei, all methyl groups of the pyrrole rings are split, whereas the central methyl group resonates as a singlet at 2.80 ppm. Also noteworthy is the quaternary ethynyl carbon which resonates at 94.4 ppm for **1**, at 119.9 ppm for **2**, and as two singlets at 94.5 and 119.8 ppm for **3**.

Electrochemistry. Cyclic voltammetry studies were carried out in deoxygenated dichloromethane containing excess tetra-*N*-butylammonium hexafluorophosphate as supporting electrolyte. Electrode processes observed for the asymmetric derivative **3** could be assigned on the basis of studies made with the symmetrical compounds **1** and **2**, and with the parent *F*-Bodipy dye. On oxidative scans, three reversible steps could be resolved with half-wave potentials ($E_{1/2}$) of 0.81, 0.91, and 1.32 V vs SCE, respectively. The first process corresponds to one-electron oxidation of the Bodipy unit,³¹ whereas the second one-electron oxidation refers to removal of an electron from the perylene unit.³² The pyrene unit undergoes one-electron oxidation at higher potentials and is responsible for the third oxidative wave.^{17,19} For **3**, it was possible to resolve two reversible, one-electron reduction processes. The first step, with $E_{1/2} = -1.54$ V vs SCE, is due to reduction of the Bodipy unit, while the second step, occurring with $E_{1/2} = -1.76$ V vs SCE, is due to reduction of the perylene group. It was not possible to observe reduction of the pyrene unit within the given electrochemical window.

The electrochemical behavior is in keeping with the relative electron densities and delocalization abilities of the polycycles. Relative to the parent *F*-Bodipy dye, it is notable that *E*-Bodipy derivatives (referring to ethynyl-substituted Bodipy dyes) are easier to oxidize by about 100 mV but more difficult to reduce by about 120 mV. It is also significant to note that these electrochemical results predict that both the HOMO and the LUMO will be centered on the Bodipy unit. Used in conjunction with the photophysical data (see later), these $E_{1/2}$ values indicate that intramolecular electron transfer from or to the Bodipy excited singlet state is thermodynamically unfavorable for both polycycles. Minor thermodynamic driving forces are available for both oxidation and reduction of the Bodipy unit by the perylene excited singlet state and for reduction of the Bodipy unit by the excited singlet state of the pyrene fragment.³³

Photophysical Studies. Absorption spectra recorded for the three new dyes display a common feature representative of the

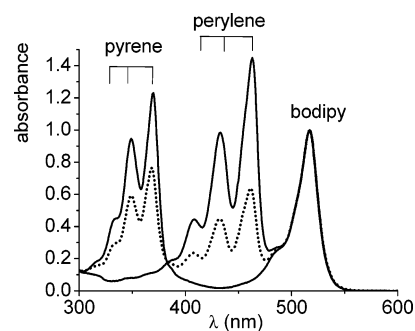


Figure 2. Absorption spectra recorded for the three dyes in MeTHF solution. Spectra for compounds **1** and **2** are shown as solid lines, with the pyrene bands being due to **1** and the perylene bands being due to **2**. The spectrum recorded for **3** is shown as a dotted line. Concentrations were ca. 10 μ M.

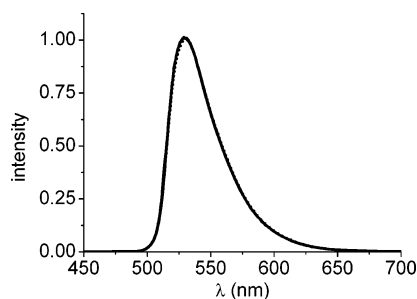


Figure 3. Normalized fluorescence spectra recorded for the three dyes in MeTHF solution. Individual spectra are overlaid to show their close comparability. The excitation wavelength was 480 nm in each case, and concentrations were around 2 μ M.

lowest-energy transition associated with the Bodipy residue (Figure 2). In each case, this feature appears as a strong $S_0 \rightarrow S_1$ transition centered (λ_{\max}) at 525 nm ($\epsilon_{\max} = 80\,000 \text{ M}^{-1} \text{ cm}^{-1}$). For **1**, there is also a weaker, broad $S_0 \rightarrow S_2$ band centered at 375 nm, but this transition is obscured in the other compounds.³⁴ Each polycycle shows a series of well-resolved absorption bands at higher energy, while **3** displays both sets of bands. There is no obvious sign of electronic coupling between the subunits, and the absorption spectrum recorded for **3** is exactly as expected on the basis of spectra recorded for **1** and **2** (Figure 2). Fluorescence, centered at 530 nm, is readily observed in fluid solution at ambient temperature and shows good mirror symmetry with the $S_0 \rightarrow S_1$ absorption transition (Figure 3). The small Stokes' shift (ca. 550 cm^{-1}) implies there is little change in geometry or polarity between ground and excited states.

The fluorescence spectra are identical throughout the series and entirely consistent with fluorescence from the Bodipy subunit (Figure 3).³⁵ For each dye, the fluorescence signal was found to decay by way of first-order kinetics with a lifetime (τ_F) of 6.5 ± 0.1 ns in deoxygenated MeTHF solution at room temperature. The fluorescence quantum yield (Φ_F) was found to be 0.90 ± 0.05 under these conditions, in each case. It is clear that the appended polycycle does not perturb the photophysical properties of the Bodipy dye. For these compounds, the radiative rate constants calculated from the Strickler–Berg expression³⁶ agree well with those derived by experiment. Both

(31) (a) Ulrich, G.; Ziessel, R. *Synlett* **2004**, 439. (b) Ulrich, G.; Ziessel, R. *J. Org. Chem.* **2004**, *69*, 2070. (c) Ulrich, G.; Ziessel, R. *Tetrahedron Lett.* **2004**, *45*, 1949. (d) Ziessel, R.; Bonardi, L.; Retaillieu, P.; Ulrich, G. *J. Org. Chem.* **2006**, *71*, 3093.

(32) Salbeck, J.; Kunkely, H.; Langhals, H.; Saalfrank, R. W.; Daub, J. *Chimia* **1989**, *43*, 6.

(33) The oxidation and reduction potentials, respectively, for the first excited singlet state of the Bodipy unit are calculated to be -1.55 and 0.82 V vs SCE. On this basis, we can rule out light-induced electron-transfer processes involving the Bodipy excited state and either of the polycycles. The reduction potential for the excited singlet state of the perylene unit is calculated to be 0.89 V vs SCE, such that this species might be expected to oxidize the Bodipy unit ($\Delta G^\circ = -0.08$ eV, ignoring electrostatic effects). The corresponding oxidation potential for the perylene unit is -1.73 V vs SCE, such that reduction of the Bodipy unit is a possibility ($\Delta G^\circ = -0.19$ eV, ignoring electrostatic effects). For pyrene, the oxidation potential for the excited singlet state is estimated to be -1.89 V vs SCE, such that, in principle, this species might be expected to reduce both the Bodipy ($\Delta G^\circ = -0.35$ eV) and perylene ($\Delta G^\circ = -0.13$ eV) units.

(34) Karolin, J.; Johansson, L. B.-A.; Strandberg, L.; Ny, T. *J. Am. Chem. Soc.* **1994**, *116*, 7801.

(35) López Arbeloa, F.; Bañuelos, J.; Martínez, V.; Arbeloa, T.; López Arbeloa, I. *Int. Rev. Phys. Chem.* **2005**, *24*, 339.

(36) Strickler, S. J.; Berg, R. A. *J. Chem. Phys.* **1962**, *37*, 814.

Φ_F and τ_F were found to be independent of temperature in deoxygenated MeTHF over the range from 300 to 80 K. Triplet state formation remains highly inefficient under these conditions, and, in the absence of a perturbing heavy-atom solvent, intersystem crossing does not compete with radiative decay of the first-excited singlet state. The triplet quantum yields are estimated from nanosecond laser flash photolysis to be less than 0.01.

The corrected fluorescence excitation spectra recorded for compounds **1–3** were found to be in excellent agreement with the corresponding absorption spectra over the range 250–530 nm. No fluorescence could be detected from either of the polycycles, and, compared to suitable reference materials, it is clear that Φ_F for the pyrene and perylene units in these compounds is $<10^{-4}$. Time-resolved fluorescence studies made with near-UV excitation confirmed that the fluorescent states associated with the polycycles have lifetimes less than 50 ps. On this basis, it appears that photons collected by the appended polycycles are transferred quantitatively to the Bodipy unit. The rate constants for intramolecular excitation energy transfer must exceed $2 \times 10^{10} \text{ s}^{-1}$. Such behavior has been noted before,^{16,17} especially with anthracene and pyrene appendages. With pyrene attached at the pseudo-meso position, it was concluded that intramolecular energy transfer occurred by a through-space process, with the overlap integral being increased due to transfer to the S_2 state localized on the Bodipy unit.¹⁷ The situation was not so clear with a series of anthracene-based dual-chromophore dyes, and both through-space and through-bond interactions were considered.¹⁶

Förster-Type Energy Transfer. The close proximity between the Bodipy and polycyclic units should favor dipole–dipole energy transfer, although the ethynylene connector could act as a good conduit for through-bond interactions.³⁷ The rate constant (k_F) for Förster-type energy transfer can be expressed in terms of eq 1,

$$k_F = \frac{(8.8 \times 10^{-25})\Phi_F K^2}{n^4 \tau_F R_{CC}^6} J_F \quad (1)$$

where

$$J_F = \frac{\int_0^\infty F_D(\nu) \epsilon_A(\nu) \nu^{-4} d\nu}{\int_0^\infty F_D(\nu) d\nu}$$

n is the refractive index of the surrounding solvent and both Φ_F and τ_F refer to the polycyclic donor when isolated from the Bodipy acceptor. Here, R_{CC} is the center-to-center separation distance between the reactants, K is their mutual orientation factor, and J_F is the spectral overlap integral.³⁸ The key factors involved in evaluating this expression are (i) identifying an appropriate reference compound with which to compute J_F , (ii) determining a realistic separation distance, and (iii) predicting the orientation factor. Given the fact that the rates of intramolecular energy transfer are very fast, the main problem concerns calculating appropriate values for K . Suitable reference compounds, used to measure Φ_F and τ_F , are available from the

Table 1. Parameters Used To Calculate the Rate Constants for Förster-Type Energy Transfer in the Three New Dyes

parameter	1 ^a	2 ^b	3 ^c
Φ_F^d	0.86	0.63	0.86
τ_F/ns^d	55	4.1	55
$R_{CC}/\text{\AA}^e$	7.7	8.5	11.5
$J_F/10^{-14} \text{ mol}^{-1} \text{ cm}^6$	1.4	13.0	3.5
$\langle K \rangle$	0.20	0.14	0.95
k_F/s^{-1}	4.7×10^{10}	1.7×10^{12}	5.0×10^{10}

^a Refers to singlet energy transfer from pyrene to the S_2 state localized on the Bodipy unit. ^b Refers to singlet energy transfer from perylene to the S_1 state localized on the Bodipy unit. ^c Refers to singlet energy transfer from pyrene to perylene. ^d Fluorescence quantum yield and lifetime for 1-trimethylsilylacetylene-pyrene and 1-triethylsilylacetylene-perylene. ^e Average center-to-center separation distance derived from the MDS runs.

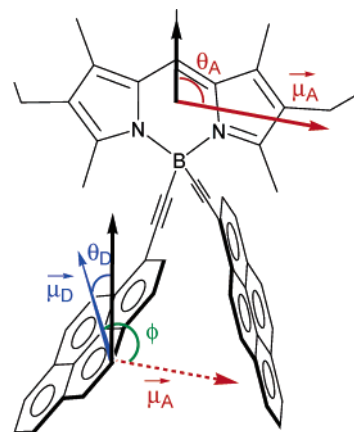


Figure 4. Illustration of the relevant transition dipole moments involved in the calculation of the orientation factor for **1**. The dipole moments μ_A and μ_D are indicated.

synthetic protocols and involve pyrene and perylene units bearing a single ethyne group at the relevant site. Photophysical properties were measured for these compounds in deoxygenated MeTHF at room temperature and are given in Table 1. The spectral overlap integral refers to the reduced fluorescence spectra (F_D) for the reference compounds, converted into wavenumber (ν), and the normalized absorption spectrum of the Bodipy unit displayed in terms of the molar absorption coefficient (ϵ_A). The derived J_F values are collected in Table 1, together with the corresponding R_{CC} values obtained from molecular modeling studies.

It is seen that the photophysical properties of the reference donors are remarkably different, especially the fluorescence lifetimes. The more extended perylene-based compound, which emits at longer wavelength, gives the larger center-to-center separation and the higher overlap integral. This latter value refers to spectral overlap with the $S_0 \rightarrow S_1$ absorption transition of the Bodipy unit for **2** but to the $S_0 \rightarrow S_2$ transition for the pyrene-based system **1**. This difference accounts for the large discrepancy between the derived J_F values. To compute the orientation factors, it is necessary to establish the geometries for the isolated molecules. Indeed, K can be expressed in terms of eq 2,

$$K = \cos \phi - 3 \cos \theta_D \cos \theta_A \quad (2)$$

where θ_D and θ_A are the angles between the transition dipole moments of the donor and acceptor, respectively, with the molecular axis and ϕ is the angle between the two dipoles (Figure 4). Information about these angles was sought from molecular modeling studies made for **1** and **2**.

(37) Harriman, A.; Zissel, R. In *Carbon-Rich Compounds*; Haley, M. M., Tykwinski, R. R., Eds.; Wiley-VCH: Weinheim, 2006; p 26.

(38) Förster, T. *Discuss. Faraday Soc.* **1959**, 27, 7.

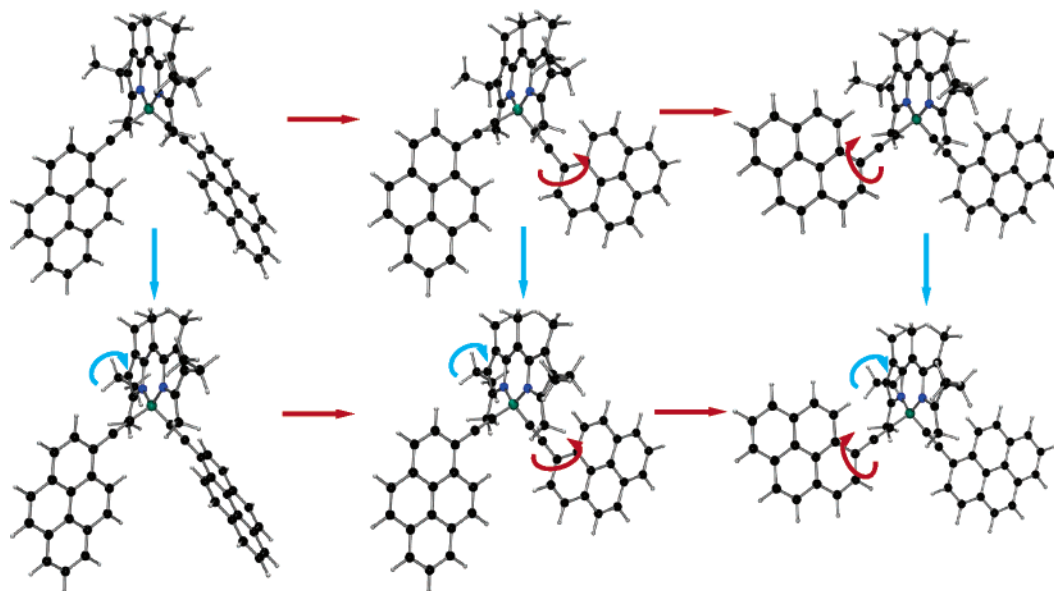


Figure 5. Representation of the major conformational exchanges available to **1** as indicated by semiempirical molecular modeling studies.

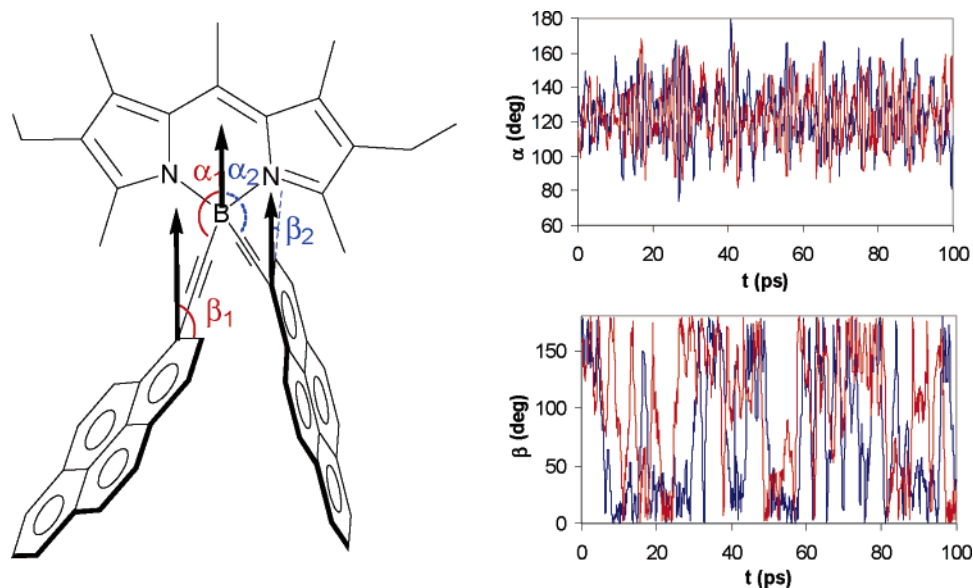


Figure 6. Left: Representation of the main torsion angles of the pyrene units with respect to the molecular axis. Right: Variation of α_i and β_i during a MDS run (red, $i = 1$; blue, $i = 2$). The torsion angles are given in absolute values.

Molecular Modeling Studies Carried Out with 1. Semiempirical molecular orbital calculations made at the AM1 level indicate that **1** adopts many different conformations that vary only slightly in energy (i.e., less than 0.1 eV). For each conformation, the energy-minimized structures for both ground and first-excited singlet states were closely comparable. Conformational heterogeneity can be considered to arise from two major internal rotations. The first grouping arises from twisting of the ethyl group (represented in blue in Figure 5) and has no observable effect on the orientation factor or separation distance. The second family of conformers arises from rotation around the connecting ethynylene group (represented in red in Figure 5) and has a profound effect on the orientation factor, but not the center-to-center separation. In particular, this rotation alters the orientation of the pyrene dipole moment with respect to the molecular axis. This effect could be seen clearly from molecular dynamics simulations.

In the MDS runs, attention was focused on the mutual orientation of the pyrene and Bodipy units. The relative orientation of the pyrene fragment can be described by the angle α and the dihedral angle β shown in Figure 6. The MDS results clearly indicate high internal flexibility around the ethynylene connector, since α and β vary over a wide range at 300 K, as shown in Figure 6. The barrier to rotation around an ethynylene connecting bond is known to be very small,³⁹ and the MDS results tend to confirm this realization. Despite the apparent stereochemical crowding caused by the bulky pyrene residue, internal rotation is facile and might be expected to take place on a time scale comparable with that of intramolecular energy transfer. The actual center-to-center separation distance remains fairly constant at 7.7 Å throughout the MDS run, and there is no indication for buckling of the indacene core, as happens for certain Bodipy derivatives.⁴⁰ Here, the structural integrity of

(39) Amini, A.; Harriman, A. *Phys. Chem. Chem. Phys.* **2003**, *5*, 1344.

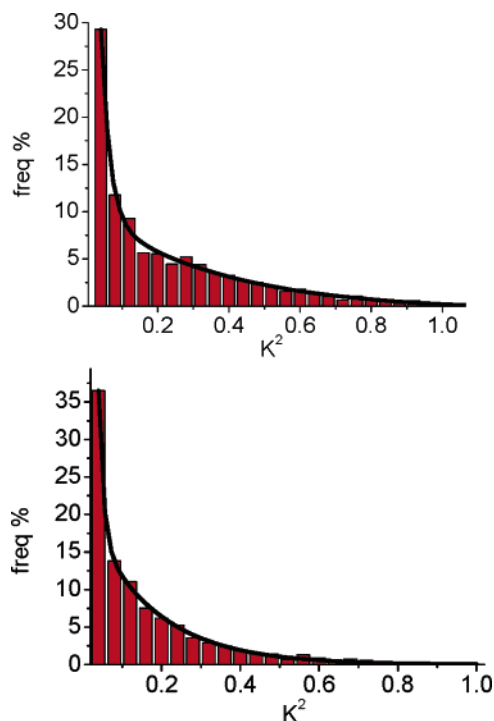


Figure 7. Statistical distribution of the orientation factor calculated from MDS runs for **1** (top panel) and **2** (bottom panel).

the compound is preserved, the indacene unit being planar, and the only serious geometrical changes are those depicted in Figure 5.

Twisting of the pyrene unit around the ethyne connector has the effect of orienting the transition dipole moment of the donor and thereby has a major influence on the size of the orientation factor. Both semiempirical calculations and the MDS studies indicate that a wide variety of conformations should be expected at ambient temperature. Although these calculations were made in vacuo, it seems unlikely that solvent molecules will completely dampen the internal oscillations. As such, K was calculated for each conformation found in the MDS runs, allowing for the frequency of occupation (Figure 7). The mean value for K is 0.2, which when used in the Förster equation predicts a mean rate of dipole–dipole energy transfer of $4.7 \times 10^{10} \text{ s}^{-1}$. This mean rate is high, given the rather limited overlap integral, and consistent with the lack of fluorescence from the pyrene unit. The Förster mechanism is insensitive to changes in temperature; again, this is in agreement with the observation that pyrene-like emission is not seen in a frozen glass at 77 K.

Molecular Modeling Studies Carried Out with 2. Semiempirical calculations also indicate that many conformations are available for **2** that differ by only minor variations in energy;

three representative conformations of **2** are given in Figure 8. Again, the computational studies found essentially the same geometry for ground and first-excited singlet states, while MDS runs confirmed the high degree of internal flexibility. The larger polycycle reduces the variation in geometry relative to **1**, but even so the orientation factor varies considerably (Figure 7). The mean K value derived from these studies is 0.14, and this allows calculation of the mean Förster rate constant as $1.7 \times 10^{12} \text{ s}^{-1}$. The higher k_F with respect to **1** (Table 1) arises from the improved spectral overlap integral since perylene fluorescence overlaps with the $S_0 \rightarrow S_1$ absorption transition localized on the Bodipy unit. The very fast rate of intramolecular energy transfer is fully consistent with the reported excitation spectra and with the noted absence of perylene-like fluorescence. The shorter singlet lifetime of the perylene-like reference compound and the enhanced J_F value compensate for the longer center-to-center distance. Excitation energy transfer from perylene to Bodipy is expected to be quantitative, as found experimentally.

Excitation Energy Transfer in 2 and 3. The absorption spectral profile characteristic of the pyrene-like unit in **1** and **3** is outside the range where the excited-state dynamics can be probed by ultrafast laser spectroscopy. As such, it has not been possible to confirm the fast rates of intramolecular energy transfer from pyrene to Bodipy, or to perylene, by direct observation. Perylene, however, absorbs at longer wavelength and can be interrogated by subpicosecond laser pulses delivered at 420 nm. The experimental setup allowed excitation of **2** in MeTHF solution with short (fwhm = 130 fs) laser pulses at 420 nm, where only the perylene unit absorbs. The course of reaction was monitored by following the rate of bleaching of the Bodipy $S_0 \rightarrow S_1$ absorption transition at 535 nm. It was observed that bleaching of the Bodipy chromophore occurred after the laser pulse and on a time scale of a few picoseconds (Figure 9). The kinetic trace did not correspond to a single-exponential curve, but the mean lifetime ($\langle\tau\rangle$) for the bleaching process was ca. 0.7 ps. This seems entirely consistent with the results of the Förster calculations and confirms the observation that the perylene unit in **2** does not fluoresce with appreciable yield. The same experiment carried out with **3** gave a mean lifetime of 0.8 ps. In each case, the bleaching curve gave a reasonable fit to stretched exponential kinetics, as expressed in terms of eq 3,

$$A(t) = A_0 e^{-(t/\langle\tau\rangle)^\alpha} \quad (3)$$

suggesting that internal rotation of the perylene unit is slower than energy transfer. Here, the stretching exponent (α) has a value of ca. 0.65 and presumably represents the distribution of conformers that do not equilibrate on the relevant time scale.

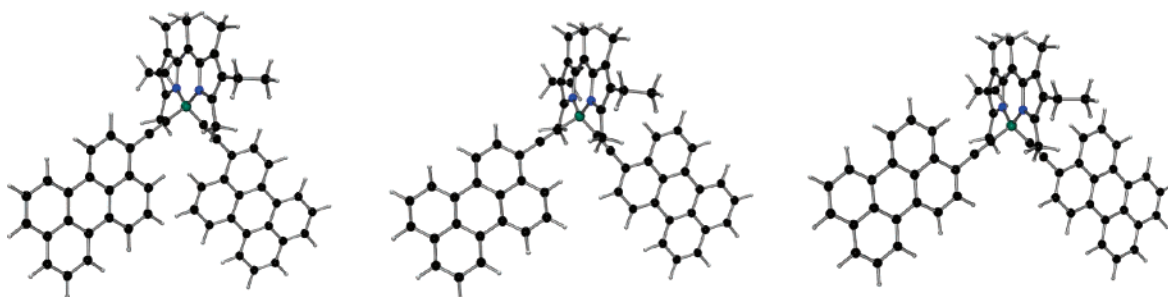


Figure 8. Representative conformations calculated for **2** by semiempirical methods.

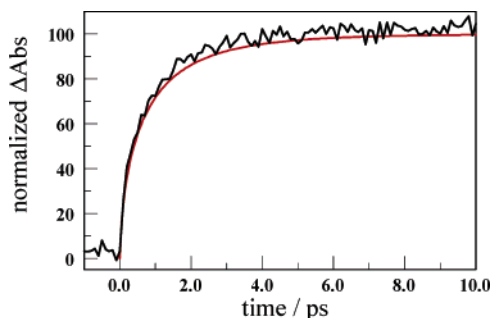


Figure 9. Typical kinetic trace showing bleaching of the Bodipy chromophore at 535 nm following laser excitation into the perylene unit for **2**. The signal has been normalized and fit to eq 3 with $\alpha = 0.65$ and $\langle\tau\rangle = 0.7$ ps. The red line is the best fit according to a linear least-squares analysis.

Concluding Remarks

The new dual-chromophore dyes introduced herein display extremely fast intramolecular energy transfer from the polycycles to the Bodipy residue. Similar behavior has been noted before for polycycles attached to the indacene core, and the rates appear comparable for the different systems. There are no obvious indications for competing intramolecular electron transfer, despite the modest thermodynamic driving forces for certain processes.³³ It is possible that the weak solvent polarity, relatively long through-space distances, and/or poor conductivity of the B atom inhibit electron transfer and thereby favor energy transfer. The ease of synthesis and, in particular, the ability to isolate asymmetrical derivatives are clear advantages of the boron-substituted dyes. We have studied both pyrene- and perylene-based systems, each connected to the boron center via a single ethyne group; these dyes can be conveniently described as *E*-Bodipy dyes so as to readily distinguish them from the more common *F*-Bodipy dyes bearing two B–F bonds. There is no reason why the synthesis cannot be extended to include other polycyclic substituents nor why cross-functionalized dyes, having additional substituents covalently linked at the indacene backbone, cannot be prepared. An interesting feature of these *E*-Bodipy dyes is that the substituent does not affect the photophysical properties of the Bodipy unit; this is in marked contrast to the corresponding *F*-Bodipy dyes, where the absorption and fluorescence spectral profiles can be tuned over a wide range. The ethynyl substituent merely functions as an ancillary

light harvester for near-UV photons. In this respect, the asymmetric derivative **3** is the most attractive dye, since it collects photons across most of the accessible spectral range. This compound fluoresces strongly when dispersed in polymeric media and acts as a highly efficient solar concentrator. It also provides for a large “virtual” Stokes’ shift, displaying several clear absorption peaks that are useful as markers for chemical sensors. The fluorescence quantum yield is independent of temperature and excitation wavelength and relatively insensitive to changes in the polarity of the surrounding medium. This dye looks to be a useful addition to the Bodipy family.

Intramolecular excitation energy transfer appears to be consistent with the Förster dipole–dipole mechanism,^{16,17} at least for the perylene-based chromophore. It is possible that the rate of energy transfer is augmented by Dexter-type through-bond interactions, given the short separation and conjugated ethynylene linker. The latter is known to be an effective bridge for electron-exchange processes.³⁷ The ability to tunnel through the central boron atom is unknown, however, and it has not been necessary to invoke the Dexter mechanism in our work.

The final point of interest concerns the possibility of setting up a cascade effect in the asymmetric derivative **3**. Here, photons absorbed by the pyrene unit can be transferred directly to the Bodipy S_2 state, in accordance with our calculations, or to the perylene unit. The latter is perfectly placed to act as an energy acceptor. The Förster-type overlap integral is high, the center-to-center separation distance is modest, and the mean orientation factor is acceptable (Table 1). Model calculations, using the reference compounds employed above, predict that the Förster-type rate of energy transfer from pyrene to perylene in **3** is on the order of $5 \times 10^{10} \text{ s}^{-1}$. As such, we might expect photons absorbed by the pyrene unit to be channeled to perylene or Bodipy units with equal probability. Unfortunately, limited experimental facilities, in terms of restricted excitation wavelengths, prevent direct observation of any such cascade effect.

Acknowledgment. We thank the EPSRC (EP/C007727/1), the CNRS, the University of Newcastle, and the Centre National de la Recherche Scientifique (CNRS) for financial support of this work.

Supporting Information Available: Complete ref 26. This material is available free of charge via the Internet at <http://pubs.acs.org>.

JA0631448

(40) Li, F.; Yang, S. I.; Ciringh, Y.; Seth, J.; Martin, C. H., III; Singh, D. L.; Kim, D.; Birge, R. R.; Bocian, D. F.; Holten, D.; Lindsey, J. S. *J. Am. Chem. Soc.* **1998**, *120*, 10001.